

# Magnetic states of iron-based superconducting compounds calculated by using GGA+ $U$ method with negative $U$

Jae Kyung Jang and Joo Yull Rhee\*

*Department of Physics, Sungkyunkwan University, Suwon 440-746, Republic of Korea*

(Dated: July 22, 2014)

## Abstract

The magnetic moments per Fe atom in high- $T_c$  iron-based superconducting compounds,  $\text{BaFe}_2\text{As}_2$  and  $\text{LaFeAsO}$  obtained from the first-principles calculation with local-spin-density approximation are much larger than those obtained from experiments. To resolve the contradictory results between theory and experiment we employed the so-called LDA+ $U$  (or more exactly GGA+ $U$ ) technique with negative  $U$  in the first-principles calculation. The calculated values with negative  $U$ ,  $-0.09$  Ry and  $-0.10$  Ry for  $\text{BaFe}_2\text{As}_2$  and  $\text{LaFeAsO}$ , respectively, are in excellent agreement with the experimental ones. By comparing the differences in  $d$ -orbital occupation numbers and spin densities calculated by using a simple GGA and GGA+ $U$  with negative  $U$ , the magnetic moments of the two compounds are found to be similar to the case of low-spin state of metamagnetic  $\text{Fe}_3\text{Al}$  alloy.

## I. INTRODUCTION

The discovery of iron-based superconductors<sup>1</sup> attracted many researchers to devote themselves into searching for possible room-temperature superconductors. Another important aspect of this system is the possibility of coexistence of seemingly mutually exclusive properties; magnetism and superconductivity. Some important issues were resolved, but there are many other aspects whose underlying physical mechanisms are still unsolved. In cases of  $\text{BaFe}_2\text{As}_2$  (referred to it as the 122-compound hereafter) and  $\text{LaFeAsO}$  (referred to it as the 1111-compound hereafter) compounds, the former undergoes the simultaneous structural, from tetragonal to orthorhombic structures, and magnetic phase transitions, from paramagnetic to antiferromagnetic (AFM) phases, at  $\sim 140$  K,<sup>2</sup> while the latter undergoes the structural phase transition from tetragonal to monoclinic (or orthorhombic<sup>3</sup>) structures at  $\sim 155$  K, and develops long-range spin-density-wave type AFM order at  $\sim 137$  K.<sup>4</sup> The magnetic moment per Fe atom of the 122-compound determined experimentally is about  $0.87 \mu_B$ ,<sup>2</sup> but the theoretical value is about  $2.6 \mu_B$ ,<sup>5</sup> and that of the 1111-compound is about  $0.36 \mu_B$  in experiment,<sup>4</sup> but is about  $1.6 \mu_B$  in theory.<sup>6</sup> For both cases, the calculated values are about 3 – 4 times overestimated over the experimental results.

At the first glance, it is usually tempted to apply the so-called ‘LDA (local-density approximation) + $U$ ’ method. This method was developed to properly describe the strongly-correlated-electron (SCE) systems which usually have very localized electrons with high angular momentum. Due to the strong on-site Coulomb repulsion among well-localized electrons, a Hubbard-type onsite repulsion is ‘manually’ included in the exchange-correlation functional during the self-consistent-field (SCF) calculation. This method was very successful for many SCE systems, however, it is well known that the onsite repulsion (i.e,  $U > 0$ ) enhances the magnetism, which is not desirable for our system. Therefore, we performed the first-principle calculations with generalized-gradient approximation (GGA)+ $U$  method, especially by using the negative  $U$ . The negative  $U$ , more exactly  $U_{\text{eff}} = U - J$ , implies that there is an effectively attractive force among  $d$ -electrons of Fe, which is very odd, however, there have been some theoretical suggestions already.<sup>7–9</sup> Moreover, the material systems, especially superconductors, with a negative effective  $U$  are not rare.

We found that, in high- $T_c$  iron-based superconducting compounds, the use of GGA+ $U$  with negative  $U$  of similar magnitudes ( $-0.09$  Ry and  $-0.10$  Ry) leads to the well-matched

values with experimental magnetic moment per Fe. We demonstrate the validity of the negative  $U$  by calculating band structures, density of states (DOS),  $d$ -electron occupation numbers and spin densities of the two compounds. Through these results, we can carefully deduce that the use of negative  $U$  in the first-principle study can give more accurate results of magnetic moments of iron-pnictide systems. More specifically, the magnetic states of the two compounds are found to be similar to the case of low-spin state of metamagnetic  $\text{Fe}_3\text{Al}$  alloy.

## II. THEORETICAL CALCULATIONS

We used the WIEN2k package<sup>10</sup> implemented with full-potential linearized-augmented-plane-wave method. The exchange-correlation functional was chosen to be GGA version of Perdew, Burke and Ernzerhof.<sup>11</sup> The spin-orbit coupling was not included. We used  $RK_{\text{max}} = 7$  and  $\sim 270$  (for the 122-compound) and  $\sim 220$  (for the 1111-compound) augmented plane waves for the basis functions. For SCF cycles we generated 1000  $\mathbf{k}$ -points in the whole Brillouin zone (BZ) corresponding to 423 (for the 122-compound) and 424 (for the 1111-compound)  $\mathbf{k}$ -points in the irreducible wedge of the BZ. After self consistency was achieved, we further increase the number of  $\mathbf{k}$ -points to 5000 in the whole BZ to obtain DOS and charge densities.

The AFM and the so-called fixed-spin-moment (FSM) calculations featured in the WIEN2k package were used. It is possible to constrain the total spin magnetic moment per unit cell to a fixed value and thus force a particular ferromagnetic solution (which may not correspond to the equilibrium). This is particularly useful for systems with several metastable magnetic solutions, where conventional spin-polarized calculation would not converge or the solution may depend on the starting density.<sup>10</sup> Since the two compounds are in the AFM state, the total magnetic moment are fixed to be zero in FSM calculations.

We included the orbital-dependent potentials, the so-called LDA+ $U$  (or GGA+ $U$ ) method.<sup>12</sup> When we calculate the effective potential  $U_{\text{eff}} = U - J$ , we set the exchange parameter  $J = 0$ , and the onsite Coulomb interaction  $U = -0.09$  Ry and  $-0.10$  Ry for the 122- and 1111-compounds, respectively. These negative  $U$ 's give very well-matched results with experimental ones. We used experimental lattice constants and magnetic structure. In the case of the 122-compound, the lattice constants were taken from Ref. 13, and magnetic

structure was taken from Ref. 2, and for the case of the 1111-compound, they were taken from Ref. 6 and Ref. 4, respectively. From now on, we will refer to this method, *i.e.* GGA+ $U$  method with negative  $U$ , as GGA- $|U|$  method.

### III. RESULTS AND DISCUSSION

The calculated magnetic moments obtained by a simple GGA calculations are about  $2.02 \mu_B/\text{Fe}$  and  $1.87 \mu_B/\text{Fe}$  for the 122- and 1111-compounds, respectively. These values are similar to those of previous publications ( $\sim 2.6 \mu_B^5$  and  $\sim 1.6 \mu_B^6$  for the 122- and 1111-compounds, respectively), however, they are still much larger than those of experiments. They were reduced to be  $0.87 \mu_B/\text{Fe}$  and  $0.38 \mu_B/\text{Fe}$  obtained by using GGA- $|U|$  method with  $U = -0.09 \text{ Ry}$  and  $-0.10 \text{ Ry}$ , respectively, which are in excellent agreement with the experimental ones.<sup>2,4</sup>

To understand these changes, the differences between the symmetry-decomposed occupation numbers of  $d$ -orbitals obtained by using the GGA and GGA- $|U|$  methods are summarized in Table I. For the 122-compound the application of negative  $U$  results in the reduction of the majority-spin  $d$ -electron occupation number by  $\sim 0.55$  and increase of the minority-spin  $d$ -electron occupation number by  $\sim 0.58$  resulting in a decrease of  $1.13 \mu_B$  of the total magnetic moment. The increase in minority-spin  $d$ -electron occupation number is more significant in the  $t_{2g}$  orbitals ( $\sim 0.37$ ) than that of the  $e_g$  orbitals ( $\sim 0.21$ ). Almost the same number of electrons are decreased in majority-spin bands for the  $t_{2g}$  and  $e_g$  bands by 0.29 and 0.26 electrons, respectively. Since the  $t_{2g}$  orbitals are composed of the  $d_{xy}$ ,  $d_{xz}$  and  $d_{yz}$  orbitals, and the  $e_g$  orbitals are composed of the  $d_{(x^2-y^2)}$  and  $d_{z^2}$  orbitals, the increased minority-spin  $d$ -electron are almost evenly distributed to all 5  $d$ -orbitals, while the electrons per orbital in the majority-spin  $e_g$  orbitals (0.13) are more severely decreased than those of the  $t_{2g}$  orbitals (0.097). This difference may cause the symmetry changes of the spin-density plots, which will be discussed later. The similar arguments can be applied to the case of the 1111-compound.

These redistributions of the symmetry-decomposed  $d$ -orbital occupation numbers ( $d$ -OONs) calculated by using the GGA- $|U|$  method is very similar to the case of those of  $\text{Fe}_3\text{Al}$  alloy upon transition from the high-spin to low-spin states.<sup>14</sup> As can be seen in the last row of Table I, the reduction of the majority-spin  $d$ -OON by  $\sim 0.54$ , and the increase of

TABLE I. Differences between the symmetry-decomposed occupation numbers of  $d$ -orbitals obtained by using GGA and GGA- $|U|$  methods ( $\Delta n_{e_g\uparrow} \equiv n_{e_g\uparrow}^{\text{GGA}-|U|} - n_{e_g\uparrow}^{\text{GGA}}$ , and so on). The change of symmetry-decomposed occupation numbers of  $d$ -orbitals upon transition from high-spin to low-spin states in Fe<sub>3</sub>Al alloy are also included for the reference.

	$\Delta n_{e_g\uparrow}$	$\Delta n_{e_g\downarrow}$	$\Delta n_{t_{2g}\uparrow}$	$\Delta n_{t_{2g}\downarrow}$
122	-0.26	0.21	-0.29	0.37
1111	-0.33	0.27	-0.39	0.43
Fe <sub>3</sub> Al	-0.26	0.10	-0.28	0.48

the minority-spin  $d$ -OON by  $\sim 0.58$ , result in a total magnetic moment decrease of  $1.22 \mu_B$  in Fe<sub>3</sub>Al alloy upon the transition from the high-spin to low-spin states. Therefore, we may think that the magnetic states of Fe atoms in the 122- and 1111-compounds are similar to the case of low-spin state of Fe<sub>3</sub>Al alloy.

There are two crystallographically different atomic sites for Fe atoms in Fe<sub>3</sub>Al alloy; *i*) Fe<sub>I</sub> atoms and *ii*) Fe<sub>II</sub> atoms. Fe<sub>I</sub> atoms are surrounded by 4 Fe<sub>II</sub> atoms and 4 Al atoms, and the surrounding atoms are located at the corners of a cube centered at the Fe<sub>I</sub> atom. On the other hand, Fe<sub>II</sub> atoms are surrounded by 8 Fe<sub>I</sub> atoms. The Fe<sub>I</sub> atom exhibits the transition from the high-spin to low-spin states at high pressure, while the magnetic moment of Fe<sub>II</sub> atom remains almost unchanged.

The 4 Al atoms surrounding a Fe<sub>I</sub> atom form a tetrahedron. It is very similar to the tetrahedral cages formed by As ligand atoms in the 122- and 1111-compounds. According to the crystal-field theory,<sup>15</sup> the 5  $d$ -orbitals will be split into the  $t_{2g}$  and  $e_g$  orbitals if the transition metal is surrounded by 4 ligand atoms forming a tetrahedral cage. Since the ligand atoms of tetrahedral cage are directly contacted with one of the lobes of  $t_{2g}$  orbitals, these orbitals have high electron-electron repulsion, resulting in a higher energy than the  $e_g$  orbitals. Since the amount of direct contact is not very large, the energy splitting is not very significant compared with the case of octahedral cages. If the energy difference ( $\Delta E_t$ ) between  $t_{2g}$  and  $e_g$  orbitals is smaller than the pairing energy ( $\Delta E_p$ ), then two electrons with opposite spins prefer to form a electron pair because the pairing reduces the total energy and, thus, the electrons do not obey the Hund's rule. The pairing reduces the magnetic moments and the transition metal-ligands complex (TMLC) is in the low-spin state. In the

majority of cases, however,  $\Delta E_t < \Delta E_p$ . Therefore, most of tetrahedral TMLCs are in the high-spin state.

The transition from high-spin state to low-spin state at high pressure can be understood by the fact that a decreased lattice constant results in pushing the bands above (below) the Fermi level ( $E_F$ ) toward the higher (lower) energy region.<sup>16,17</sup> It implies that  $\Delta E_t$  increases as the pressure is applied, favoring the pairing of electrons and, hence, the transition to the low-spin state

In our case, the situation is not that simple. Figure 1 clearly exhibits the tendency of redistribution of the symmetry-decomposed  $d$ -OONs of both compounds. Majority-spin bands move upward, while minority-spin bands move downward for both  $t_{2g}$  and  $e_g$  orbitals, and all  $t_{2g}$  and  $e_g$  orbitals are split into two band groups for both majority- and minority-spin bands. To show this tendency of redistribution of the symmetry-decomposed  $d$ -OONs more clearly a schematic diagrams of symmetry decomposed Fe  $d$ -DOS of metamagnetic Fe<sub>3</sub>Al alloy is presented in Fig 2. For the  $e_g$  majority-spin bands only the upper-band group is located near  $E_F$ , while the both band groups of minority-spin bands are far from  $E_F$ . Therefore,  $d$ -OONs of  $e_g$  orbitals do not change significantly for majority spin, while there are almost no change in  $d$ -OONs of  $e_g$  orbitals for minority spin upon transition to the low-spin state. The situation of the case of  $t_{2g}$  orbitals is quite different from that of the  $e_g$  orbitals. The upper majority-spin bands of  $t_{2g}$  orbitals are located just below  $E_F$ , and the lower minority-spin bands of  $t_{2g}$  orbitals are located just above  $E_F$  for the high-spin state. Upon transition to the low-spin state,  $d$ -OONs for majority-spin (minority-spin)  $t_{2g}$  orbitals decreases (increases) significantly, resulting in a significant reduction of magnetic moment.

This redistributions of  $d$ -OONs can be clearly manifested in spin-density plots. Before discussing the spin densities of the Fe-based pnictide compounds, we present spin-density plots for the high-spin and low-spin states of metamagnetic Fe<sub>3</sub>Al alloy in Fig. 3. The distribution of spin density plotted on the (110) plane (left panel) around the Fe<sub>I</sub> atom is symmetric and exhibits no significant directionality in the high-spin state, while that for the low-spin state exhibits a strong directionality. Especially, the strong directionality appears along the  $z$ -axis. For the high-spin state  $d$ -OONs of five  $d$ -orbitals are almost identical to each other, while those of  $e_g$  orbitals are significantly smaller than those of  $t_{2g}$  orbitals for the low-spin state. Therefore, the directionality appeared along the  $z$ -axis is evident, reflecting the deficiency of  $d_{z^2}$  orbital in the low-spin state. The same arguments can be applied to

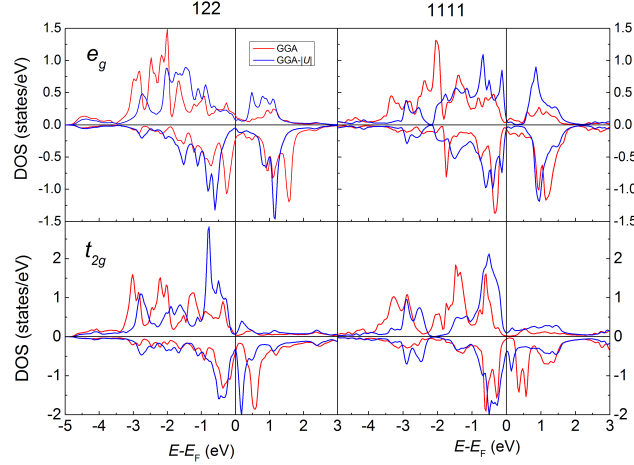


FIG. 1. (Color online.) Symmetry-decomposed Fe  $d$ -DOS of the 122- and 1111-compounds.

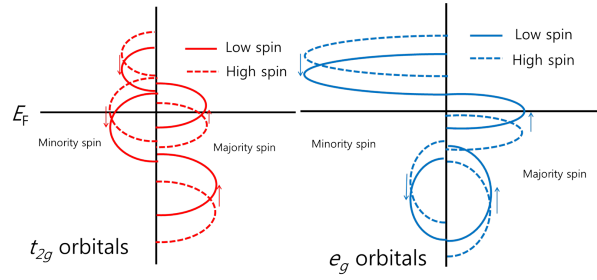


FIG. 2. (Color online.) Schematic diagrams of symmetry-decomposed Fe  $d$ -DOS of metamagnetic  $\text{Fe}_3\text{Al}$  alloy.

the plots on the (001)-plane (see the right panel of Fig. 3). In the low-spin state the spin density exhibits strong directionality along the  $x$ - and  $y$ -axes, reflecting the deficiency of  $d_{(x^2-y^2)}$  orbitals.

To see if the same trend can be found in the Fe-based pnictide compounds, Fig. 4 presents the spin-density plots of the 1111-compound on the (010) and (100) planes. Unlike the case of the metamagnetic  $\text{Fe}_3\text{Al}$  alloy, in calculations with simple GGA there is no symmetric distribution of spin density on the (010) plane, in which the magnetization is in the plane. In the  $\text{GGA}-|U|$  calculation the spin density exhibits clear 4-fold symmetry, while it is slightly 2-fold in the simple GGA calculation. For the (100) plane, in which the magnetization is out of the plane, the situation becomes opposite. It exhibits almost perfect 4-fold symmetry in the simple GGA calculation, while it becomes slightly 2-fold symmetric in the  $\text{GGA}-|U|$

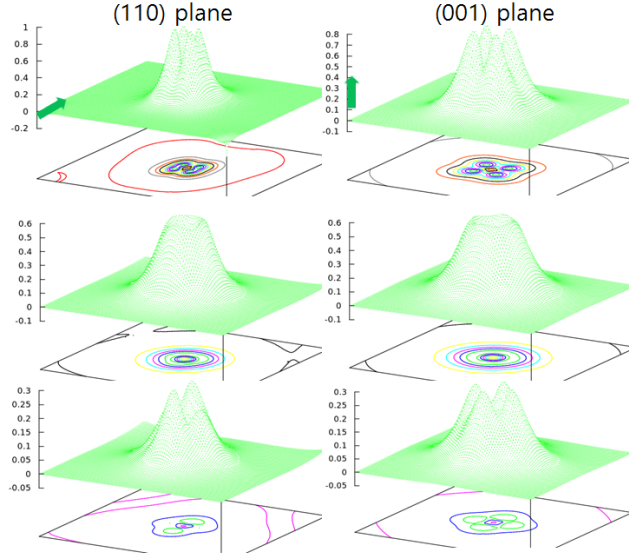


FIG. 3. (Color online.) Spin-density plots of the  $\text{Fe}_3\text{Al}$  alloy on the (110) and (001) planes for (top) fictitious  $\text{Fe}_2\text{Al}$  alloy (see text), (middle) for high-spin state, and (bottom) for the low-spin state. Thick arrows indicate the direction of magnetization.

calculation. Very similar arguments can be applied to the case of the 122-compound.

Since the transition from high-spin state to low-spin state occurs at high pressure, the distance between the Fe atom and ligand atom,  $d_{\text{Fe-Lig.}}$ , may play a crucial role. For the  $\text{Fe}_3\text{Al}$  alloy  $d_{\text{Fe-Lig.}} = 4.48$  a.u.<sup>14</sup> in the low-spin state, while those for the 122- and 1111-compounds are 4.53 a.u. and 4.46 a.u., respectively. Since all  $d_{\text{Fe-Lig.}}$ 's are in almost the same distances, we calculated the spin densities of a fictitious 1111-compound with the expanded lattice constant, bearing  $d_{\text{Fe-Lig.}} = 4.7$  a.u., which is the same as that of  $\text{Fe}_3\text{Al}$  alloy in the ambient pressure. As can be seen in the top row of Fig. 4, the spin-density plots do not exhibit a symmetric distribution of spin density. Rather, it is more 2-fold symmetric for the (010) plane and more 4-fold symmetric for the (100) plane. Although there are only 4 As atoms, forming a tetrahedral cage, around the Fe atoms in Fe-based pnictide compounds, there are 4 Al atoms, forming a tetrahedral cage, *plus* 4  $\text{Fe}_{\text{II}}$  atoms, also forming a tetrahedral cage, around the  $\text{Fe}_{\text{I}}$  atom. To compare the results of the  $\text{Fe}_3\text{Al}$  alloy with those of Fe-based pnictide compounds, it is necessary to remove the effects of surrounding 4  $\text{Fe}_{\text{II}}$  atoms. Therefore, we calculated the spin density of another fictitious  $\text{Fe}_2\text{Al}$  alloy, in which the  $\text{Fe}_{\text{II}}$  atoms are removed from the  $\text{Fe}_3\text{Al}$  alloy. The results are



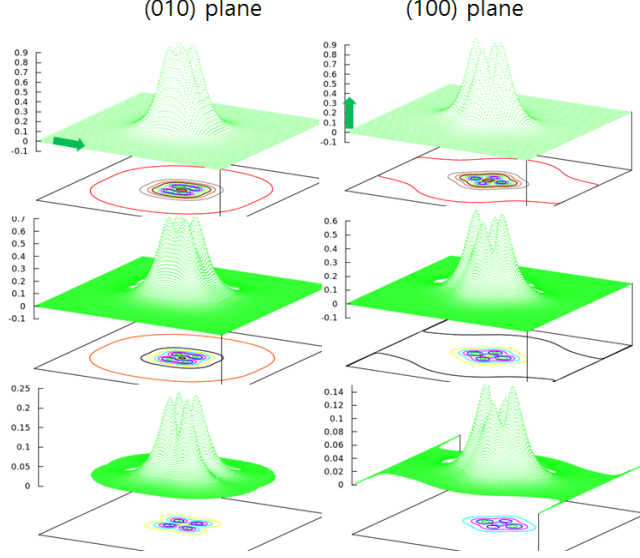


FIG. 4. (Color online.) Spin-density plots of the 1111-compound on the (010) and (100) planes for (top) fictitious compound with expanded lattice constant (see text), (middle) for a simple GGA calculation, and (bottom) for GGA- $|U|$  calculation. Thick arrows indicate the direction of magnetization.

almost identical to those of the fictitious 1111-compound with the expanded lattice constant (see the top row of Fig. 3).

The symmetric distribution of spin density in the high-spin state of the  $\text{Fe}_3\text{Al}$  alloy can be attributed to the existence of 4  $\text{Fe}_{\text{II}}$  atoms. Since the 4  $\text{Fe}_{\text{II}}$  atoms form another tetrahedral cage, they can attract spin density into themselves from the  $\text{Fe}_{\text{I}}$  atom, resulting in a symmetric distribution of spin density in the high-spin state. The effects of the existence of 4  $\text{Fe}_{\text{II}}$  atoms can be further manifested by the fact that the symmetry directions in the spin-density plot on the (001) plane for the low-spin state are  $45^\circ$  rotated from those of fictitious  $\text{Fe}_2\text{Al}$  alloy.

According to our calculational results, the LDA, GGA or GGA+ $U$  with positive  $U$  can not properly predict the magnetic states of the Fe-based pnictide superconductors. Rather, the GGA- $|U|$  method can. In Ref. 9 it was argued that the negative  $U$  correction can be considered as an unexpectedly well screening on  $d$ -orbitals in Fe atoms. If the screening is strong enough or over, then we can reach a situation that the intra-band repulsion becomes smaller than the inter-band one. In such a case, an effectively attractive force may result in.

#### IV. SUMMARY

We have calculated the electronic structures, DOS, occupation numbers and spin-density of  $3d$  Fe of  $\text{BaFe}_2\text{As}_2$  and  $\text{LaFeAsO}$  in the orthorhombic, AFM phases by using GGA and  $\text{GGA}-|U|$ . We found that, in high- $T_c$  iron-based superconducting compounds, the use of GGA with negative  $U$  with similar values ( $-0.09$  Ry and  $-0.10$  Ry) give the well-matched results with experimental magnetic moment per Fe atom. By comparing the differences of DOS, symmetry-decomposed  $d$ -OONs and spin densities between simple GGA and  $\text{GGA}-|U|$  calculations, the magnetic state of the iron-based pnictide compounds are very similar to the case of the low-spin state of metamagnetic  $\text{Fe}_3\text{Al}$  alloy. To further address the validity of negative  $U$  more researches, such as direct calculation of the onsite Coulomb interaction  $U$  and the exchange interaction  $J$  from the first-principles calculations, are needed.

#### ACKNOWLEDGMENTS

This research was supported by the Basic Science Research Program through the National Research Foundation of Korea (NRF) funded by the Ministry of Education, Science and Technology (2011-0023423). This work was also supported by the Faculty Research Fund, Sungkyunkwan University, 2006.

---

\* rheejy@skku.edu

- <sup>1</sup> Y. Kamihara, T. Watanabe, M. Hirano, and H. Hosono, J. Am. Chem. Soc. **130**, 3296 (2008).
- <sup>2</sup> Q. Huang, Y. Qiu, W. Bao, M. A. Green, J. W. Lynn, Y. C. Gasparovic, T. Wu, G. Wu, and X. H. Chen, Phys. Rev. Lett. **101**, 257003 (2008).
- <sup>3</sup> T. Yildirim, Phys. Rev. Lett. **101**, 057010 (2008).
- <sup>4</sup> C. de la Cruz, Q. Huang, J. W. Lynn, J. Li, W. R. Li, J. L. Zarestky, H. A. Mook, G. F. Chen, J. L. Luo, N. L. Wang, and P. Dai, Nature **453**, 899 (2008).
- <sup>5</sup> E. Aktürk and S. Ciraci, Phys. Rev. B **79**, 184523 (2009).
- <sup>6</sup> T. Nomura, S. W. Kim, Y. Kamihara, M. Hirano, P. V. Sushko, K. Kato, M. Takata, A. L. Shluger, and H. Hosono, Supercond. Sci. Techn. **21**, 125028 (2008).
- <sup>7</sup> R. Micnas, J. Ranninger, and S. Robaszkiewicz, Rev. Mod. Phys. **62**, 113 (1990).

- <sup>8</sup> I. Hase and T. Yanagisawa, Phys. Rev. B **76**, 174103 (2007).
- <sup>9</sup> H. Nakamura, N. Hayashi, N. Nakai, M. Okumura, and M. Machida, Physica C: Superconductivity **469**, 908 (2009).
- <sup>10</sup> P. Blaha, K. Schwarz, G. K. H. Madsen, D. Kvasnicka, and J. Luitz, *WIEN2K, An Augmented Plane Wave + Local Orbitals Program for Calculating Crystal Properties* (Karlheinz Schwarz, Techn. Universität Wien, Austria, 2001).
- <sup>11</sup> J. P. Perdew, K. Burke, and M. Ernzerhof, Phys. Rev. Lett. **77**, 3865 (1996).
- <sup>12</sup> V. I. Anisimov, I. V. Solovyev, M. A. Korotin, M. T. Czyżyk, and G. A. Sawatzky, Phys. Rev. B **48**, 16929 (1993).
- <sup>13</sup> M. Rotter, M. Tegel, and D. Johrendt, Phys. Rev. Lett. **101**, 107006 (2008).
- <sup>14</sup> J. Y. Rhee and B. N. Harmon, Phys. Rev. B **70**, 094411 (2004).
- <sup>15</sup> Wikipedia, “Crystal field theory — wikipedia, the free encyclopedia,” (2014), [Online; accessed 6-July-2014].
- <sup>16</sup> J. Y. Rhee, Y. V. Kudryavtsev, Y. P. Lee, and K. W. Kim, J. Korean Phys. Soc. **36**, 404 (2000).
- <sup>17</sup> J. Y. Rhee, J. Korean Phys. Soc. **43**, 1091 (2003).